



Computing the Maslov index of solitary waves, Part 2: Phase space with dimension greater than four

Frédéric Chardard^{a,*}, Frédéric Dias^{b,c}, Thomas J. Bridges^d

^a UMPA (Site Monod), École Normale Supérieure de Lyon, CNRS UMR 5669, Université de Lyon, 46, allée d'Italie, 69007 Lyon, France

^b Centre de Mathématiques et de Leurs Applications, École Normale Supérieure de Cachan, 61 avenue du Président Wilson, 94235 Cachan cedex, France

^c School of Mathematical Sciences, University College Dublin, Belfield, Dublin, 4, Ireland

^d Department of Mathematics, University of Surrey, Guildford GU2 7XH, England, United Kingdom

ARTICLE INFO

Article history:

Received 15 June 2010

Received in revised form

9 May 2011

Accepted 10 May 2011

Available online 17 May 2011

Communicated by B. Sandstede

Keywords:

Solitary waves

Stability

Maslov index

Hamiltonian systems

Evans function

Long-wave–short-wave resonance

ABSTRACT

This paper extends the theory of the Maslov index of solitary waves in Part 1 to the case where the phase space is of dimension greater than four. The starting point is Hamiltonian PDEs, in one space dimension and time, whose steady part is a Hamiltonian ODE with a phase space of dimension six or greater. This steady Hamiltonian ODE is the main focus of the paper. Homoclinic orbits of the steady ODE represent solitary waves of the PDE, and one of the properties of the homoclinic orbits is the Maslov index. We develop formulae for the Maslov index, the Maslov angle and its subangles, in an exterior algebra framework, and develop numerical algorithms to compute them. In addition, a new numerical approach based on a discrete QR algorithm is proposed. The Maslov index is of interest for classifying solitary waves and as an indicator of stability or instability of the solitary wave in the time-dependent problem. The theory is applied to a class of reaction–diffusion equations, the longwave–shortwave resonance equations and the seventh-order KdV equation.

© 2011 Elsevier B.V. All rights reserved.

1. Introduction

Hamiltonian evolution equations in one space dimension, such as the nonlinear Schrödinger (NLS) equation, the family of n th order Korteweg–de Vries (KdV) equations, and longwave–shortwave resonance (LW–SW) equations, have the property that their steady part is a finite-dimensional Hamiltonian system. For such systems, solitary wave solutions can be characterized as homoclinic orbits of a Hamiltonian ordinary differential equation (ODE). The spectral problem associated with the linearization about a given homoclinic orbit, in the time-dependent equations, then leads to a parameter-dependent family of linear Hamiltonian systems. The advantage of these Hamiltonian structures is that the linear and nonlinear Hamiltonian systems have global geometric properties that aid in proving the existence of the basic solitary wave and in understanding its stability as a solution of the time-dependent equation. Our interest in this paper is in a particular geometric invariant – the Maslov index of homoclinic orbits. This paper is a continuation of Chardard et al. [1] (hereafter Part 1). It extends the

theory of Jones [2], Bose & Jones [3] and Part 1 to cases where the phase space of the steady Hamiltonian ODE has dimension six or greater.

Once the solitary wave solution is known, analytically or numerically, it is the linearization about that solitary wave which encodes the Maslov index. Therefore, the starting point for developing the theory is the following class of parameter-dependent Hamiltonian systems

$$\mathbf{J}\mathbf{w}_x = \mathbf{B}(x, \lambda)\mathbf{w}, \quad \mathbf{w} \in \mathbb{R}^{2n}, \quad x \in \mathbb{R}, \quad \lambda \in \mathbb{R}, \quad (1.1)$$

where \mathbf{J} is the standard symplectic operator on \mathbb{R}^{2n}

$$\mathbf{J} = \begin{bmatrix} \mathbf{0} & -\mathbf{I} \\ \mathbf{I} & \mathbf{0} \end{bmatrix}, \quad (1.2)$$

and $\mathbf{B}(x, \lambda)$ is a symmetric matrix depending smoothly on x and λ . Let

$$\mathbf{A}(x, \lambda) = \mathbf{J}^{-1}\mathbf{B}(x, \lambda). \quad (1.3)$$

The fact that $\mathbf{A}(x, \lambda)$ is obtained from the linearization about a solitary wave suggests the following asymptotic property. It is assumed throughout the paper that

$$\mathbf{A}_\infty(\lambda) = \lim_{x \rightarrow \pm\infty} \mathbf{A}(x, \lambda), \quad (1.4)$$

and that $\mathbf{A}_\infty(\lambda)$ is strictly hyperbolic for an open set of λ values that includes 0.

* Corresponding author. Tel.: +33 4 72 72 81 88; fax: +33 4 72 72 81 80.

E-mail addresses: frederic.chardard@umpa.ens-lyon.fr,
chardard@cmla.ens-cachan.fr (F. Chardard).

The Maslov index is a winding number associated with paths of Lagrangian planes of solutions of (1.1), in particular the unstable space, i.e. the space of solutions which decays at $-\infty$ when $\mathbf{A}_\infty(\lambda)$ is hyperbolic. We present formulae for different representations of the Maslov index for Lagrangian planes on $\bigwedge^n(\mathbb{R}^{2n})$ for any n , and use the numerical algorithm of Part 1 to compute it. It works in principle in any dimension. However, since we use an exterior algebra representation, the dimension of $\bigwedge^n(\mathbb{R}^{2n})$ increases rapidly with n and so the algorithm is most effective for low-dimensional systems. In this paper formulae are presented for any dimension and numerical results for a phase space of dimension six.

In addition, a new algorithm based on a discrete QR splitting is proposed. When $n = 2$ the exterior algebra frame is clearly faster than the QR method; its computation time is about the same when $n = 3$ but for $n > 3$ the QR method appears to be faster.

The computational framework for the Maslov index is illustrated by application to three examples. The first example is the fully coupled longwave–shortwave resonance equation from the theory of water waves, which consists of an NLS equation coupled to a KdV equation, generalizing results from [4,1]. The second example is a sixth-order system that arises in the linearization about the coupled reaction–diffusion equations. The third example is the seventh-order KdV equation, which has the property that the steady part is a Hamiltonian system on a phase space of dimension six, and extends the results on the fifth-order KdV in [1].

2. Linear Hamiltonian systems and Lagrangian subspaces

Let

$$\mathbf{W} = [\mathbf{w}_1 \mid \cdots \mid \mathbf{w}_n] \in \mathbb{R}^{2n \times n}, \quad (2.1)$$

where the linearly independent columns $\{\mathbf{w}_1, \dots, \mathbf{w}_n\}$ span an n -dimensional subspace. This subspace is Lagrangian if

$$\mathbf{W}^T \mathbf{J} \mathbf{W} = \mathbf{0}, \quad (2.2)$$

or columnwise

$$\langle \mathbf{J} \mathbf{w}_i, \mathbf{w}_j \rangle = 0, \quad \forall i, j = 1, \dots, n,$$

where $\langle \cdot, \cdot \rangle$ is a standard inner product on \mathbb{R}^{2n} .

Now suppose the subspace (2.1) depends on (x, λ) and satisfies the differential equation (1.1),

$$\mathbf{J} \mathbf{W}_x = \mathbf{B}(x, \lambda) \mathbf{W}. \quad (2.3)$$

The differential equation preserves Lagrangian subspaces since

$$\frac{d}{dx} (\mathbf{W}^T \mathbf{J} \mathbf{W}) = -\mathbf{W}^T \mathbf{B} \mathbf{W} + \mathbf{W}^T \mathbf{B} \mathbf{W} = \mathbf{0}.$$

Hence if the initial data $\mathbf{W}(x, \lambda)|_{x=x_0}$ is Lagrangian, the path $\mathbf{W}(x, \lambda)$ is Lagrangian for all $x > x_0$.

A Lagrangian subspace can also be represented by a *Lagrangian frame* [5]: a $2n \times n$ matrix of rank n

$$\mathbf{W} = \begin{pmatrix} \mathbf{U} \\ \mathbf{V} \end{pmatrix}, \quad (2.4)$$

where condition (2.2) requires the $n \times n$ matrices \mathbf{U} and \mathbf{V} to satisfy

$$\mathbf{V}^T \mathbf{U} = \mathbf{U}^T \mathbf{V}. \quad (2.5)$$

This identity implies that

$$(\mathbf{U} - i\mathbf{V})^T (\mathbf{U} + i\mathbf{V}) = \mathbf{U}^T \mathbf{U} + \mathbf{V}^T \mathbf{V}.$$

Hence if $\mathbf{R} = \sqrt{\mathbf{U}^T \mathbf{U} + \mathbf{V}^T \mathbf{V}}$, which is well defined and symmetric since the argument is positive definite, then

$$\mathbf{Q} = \mathbf{Q}_1 + i\mathbf{Q}_2 := (\mathbf{U} + i\mathbf{V})\mathbf{R}^{-1},$$

is unitary. The determinant of a unitary matrix lies on the unit circle. It is this observation that leads to a definition of the *Maslov angle* of a fixed Lagrangian subspace \mathbf{W} ,

$$e^{i\kappa} = \frac{\det[\mathbf{U} - i\mathbf{V}]}{\det[\mathbf{U} + i\mathbf{V}]} \quad (2.6)$$

For an (x, λ) -path of Lagrangian subspaces the angle is

$$e^{i\kappa(x, \lambda)} = \frac{\det[\mathbf{U}(x, \lambda) - i\mathbf{V}(x, \lambda)]}{\det[\mathbf{U}(x, \lambda) + i\mathbf{V}(x, \lambda)]}. \quad (2.7)$$

Suppose that $\mathbf{W}(x, \lambda)$, for fixed λ and $a \leq x \leq b$, is a smooth path of Lagrangian subspaces. If the path is a loop: $\mathbf{W}(b, \lambda) = \mathbf{W}(a, \lambda)$, then there is an integer associated with the path: the number of times the induced path on S^1 , $e^{i\kappa(x, \lambda)}$, encircles the origin. This integer is the *Maslov index* of the path

$$\text{Maslov}(\kappa) := \frac{\kappa(b, \lambda) - \kappa(a, \lambda)}{2\pi}. \quad (2.8)$$

When (1.1) is obtained from the linearization about a homoclinic orbit, the Lagrangian subspace represents the stable or unstable subspace of the linearization. Hence direct numerical integration of (2.3) is unstable. The remedy for this is to integrate using exterior algebra, or integrating using discrete or continuous orthogonalization. The exterior algebra approach was developed in [4,1] for the case of $n = 2$. Here the necessary details for generalizing to $n > 2$ are sketched. The use of discrete orthogonalization for computing the Maslov index is new, and the details are given in Section 9.

3. Integrating (1.1) on exterior algebra spaces

Let $\mathbf{e}_1, \dots, \mathbf{e}_{2n}$ be the standard basis for \mathbb{R}^{2n} . Then

$$\{\mathbf{e}_{k_1} \wedge \cdots \wedge \mathbf{e}_{k_n} \mid k_1, \dots, k_n \in \{1, \dots, 2n\}\},$$

is a basis for $\bigwedge^n(\mathbb{R}^{2n})$. Any element $\mathbf{Z} \in \bigwedge^n(\mathbb{R}^{2n})$ can be expressed in terms of this basis. There is then a standard way to construct the differential equation induced on $\bigwedge^n(\mathbb{R}^{2n})$ by (1.1) leading to

$$\mathbf{Z}_x = \mathbf{A}^{(n)}(x, \lambda) \mathbf{Z}, \quad \mathbf{Z} \in \bigwedge^n(\mathbb{R}^{2n}). \quad (3.9)$$

The principal issue is the construction of the matrix $\mathbf{A}^{(n)}$ [6,1]. In this section a new construction of this matrix is given using the multi-alternate product following [7]. The *bi*-alternate product is now widely used in bifurcation theory (e.g. Govaerts [8]). There is not much in the literature on the *multi*-alternate product, but the basics of the theory were worked out over 100 years ago by Stéphanos [9,10].

The multi-alternate product of matrices is defined as follows. Let E and F be two vector spaces. Let $\mathbf{M}_1, \mathbf{M}_2, \dots, \mathbf{M}_k$ be linear maps from E to F . Then, the k th-alternate product is a mapping

$$(\mathbf{M}_1, \mathbf{M}_2, \dots, \mathbf{M}_k) \mapsto \mathbf{M}_1 \odot \mathbf{M}_2 \odot \cdots \odot \mathbf{M}_k : \bigwedge^k E \rightarrow \bigwedge^k F,$$

defined by

$$\begin{aligned} \mathbf{M}_1 \odot \mathbf{M}_2 \odot \cdots \odot \mathbf{M}_k (\mathbf{a}_1 \wedge \mathbf{a}_2 \wedge \cdots \wedge \mathbf{a}_k) \\ = \frac{1}{k!} \sum_{\sigma \in \Sigma_k} \mathbf{M}_{\sigma(1)} \mathbf{a}_1 \wedge \mathbf{M}_{\sigma(2)} \mathbf{a}_2 \wedge \cdots \wedge \mathbf{M}_{\sigma(k)} \mathbf{a}_k \end{aligned}$$

where Σ_k is the set of permutations of $\{1, \dots, k\}$. Let $(\mathbf{e}_1, \dots, \mathbf{e}_n)$ and $(\mathbf{f}_1, \dots, \mathbf{f}_n)$ be bases of E and F . Then

$$\begin{aligned} \{\mathbf{e}_{i_1} \wedge \cdots \wedge \mathbf{e}_{i_k}, 1 \leq i_1 < \cdots < i_k \leq n\} \quad \text{and} \\ \{\mathbf{f}_{i_1} \wedge \cdots \wedge \mathbf{f}_{i_k}, 1 \leq i_1 < \cdots < i_k \leq m\}, \end{aligned}$$

are bases for $\bigwedge^k E$ and $\bigwedge^k F$. The entries of the matrix of the multi-alternate product in these bases is

$$(\mathbf{M}_1 \odot \cdots \odot \mathbf{M}_k)_{\substack{1 \leq i_1 < \cdots < i_k \leq n, \\ 1 \leq j_1 < \cdots < j_k \leq n}} = \frac{1}{k!} \sum_{\sigma \in \Sigma_n} \begin{vmatrix} (\mathbf{M}_{\sigma(1)})_{i_1 j_1} & (\mathbf{M}_{\sigma(1)})_{i_1 j_2} & \cdots & (\mathbf{M}_{\sigma(1)})_{i_1 j_k} \\ (\mathbf{M}_{\sigma(2)})_{i_2 j_1} & (\mathbf{M}_{\sigma(2)})_{i_2 j_2} & \cdots & (\mathbf{M}_{\sigma(2)})_{i_2 j_k} \\ \vdots & \vdots & \ddots & \vdots \\ (\mathbf{M}_{\sigma(k)})_{i_k j_1} & (\mathbf{M}_{\sigma(k)})_{i_k j_2} & \cdots & (\mathbf{M}_{\sigma(k)})_{i_k j_k} \end{vmatrix}.$$

The induced matrix $\mathbf{A}^{(n)}$ in terms of the multi-linear product is then

$$\mathbf{A}^{(n)} = n(\mathbf{A} \odot \mathbf{I} \odot \cdots \odot \mathbf{I}). \quad (3.10)$$

A formula for the induced matrix, in terms of the standard basis for $\bigwedge^k(\mathbb{R}^{2n})$, for any k is

$$(\mathbf{A}^{(k)})_{\substack{1 \leq i_1 < \cdots < i_k \leq 2n, \\ 1 \leq j_1 < \cdots < j_k \leq 2n}} = \begin{cases} 0 & \text{if Card}(\{i_1, \dots, i_k\} \cup \{j_1, \dots, j_k\}) > k+1 \\ (-1)^{r+s} a_{i_r j_s} & \text{if } \{i_r, j_s\} = \{i_1, \dots, i_k\} \Delta \{j_1, \dots, j_k\} \\ \sum_{r=1}^k a_{i_r, i_r} & \text{if } \{i_1, \dots, i_k\} = \{j_1, \dots, j_k\} \end{cases} \quad (3.11)$$

with $V \Delta W = (V \cup W) - (V \cap W)$. For numerical computations, it is natural to use a mono-index implementation rather than a multi-index one. Normally, the C_{2n}^k multi-indexes are numbered following the lexical ordering: let $1 \leq i_1 < \cdots < i_k \leq 2n$ and $1 \leq j_1 < \cdots < j_k \leq 2n$. It is said that

$$\{i_1, \dots, i_k\} < \{j_1, \dots, j_k\} \quad \text{if and only if } \exists \alpha \mid i_1 = j_1, \dots, i_{\alpha-1} = j_{\alpha-1} \text{ and } i_\alpha < j_\alpha.$$

An explicit expression for $\mathbf{A}^{(n)}$ in the standard basis when $n = 3$ is given in the Appendix of [11].

3.1. Reversibility and the multi-alternate product

Another advantage of the multi-alternate product is that it provides the natural setting for constructing the induced reversors on $\bigwedge^n(\mathbb{R}^{2n})$ when $\mathbf{A}(x, \lambda)$ is reversible.

Suppose that the linear system (1.1) is reversible: there exists a linear transformation $\mathbf{R} : \mathbb{R}^{2n} \rightarrow \mathbb{R}^{2n}$ such that

$$\mathbf{R}\mathbf{J} = -\mathbf{J}\mathbf{R} \quad \text{and}$$

$$\mathbf{R}\mathbf{B}(-x, \lambda) = \mathbf{B}(x, \lambda)\mathbf{R}, \quad \mathbf{R}^{-1} = \mathbf{R}, \quad (3.12)$$

or in terms of $\mathbf{A}(x, \lambda)$ in (1.3)

$$\mathbf{R}\mathbf{A}(-x, \lambda) = -\mathbf{A}(x, \lambda)\mathbf{R}. \quad (3.13)$$

For a linear operator on \mathbb{R}^{2n} define the operation of inducing a mapping on $\bigwedge^n(\mathbb{R}^{2n})$ by

$$\bigwedge^n(\mathbf{A}) := \mathbf{A}^{(n)}. \quad (3.14)$$

It is immediate from the definition that

$$\bigwedge^n(\mathbf{A}(-x, \lambda)) := \mathbf{A}^{(n)}(-x, \lambda). \quad (3.15)$$

Since reversibility will not play a role in this paper, restrict attention to the case $n = 2$ to illustrate the construction of induced reversors. An application of the Maslov index where reversibility is important is presented in [12].

The bialternate has the following interesting property (cf. Proposition 14 on page 40 of [7])

$$\bigwedge^2(\mathbf{Q}^{-1}\mathbf{A}\mathbf{Q}) = (\mathbf{Q} \odot \mathbf{Q})^{-1} \bigwedge^2(\mathbf{A})(\mathbf{Q} \odot \mathbf{Q}). \quad (3.16)$$

From this identity and (3.15)

$$\begin{aligned} -\mathbf{A}^{(2)}(-x, \lambda) &= -\bigwedge^2(\mathbf{A}(-x, \lambda)) \\ &= \bigwedge^2(\mathbf{R}^{-1}\mathbf{A}(x, \lambda)\mathbf{R}) \quad (\text{using (3.13) and } \mathbf{R}^{-1} = \mathbf{R}) \\ &= (\mathbf{R} \odot \mathbf{R})^{-1} \bigwedge^2(\mathbf{A}(x, \lambda))(\mathbf{R} \odot \mathbf{R}) \quad (\text{using (3.16)}) \\ &= (\mathbf{R} \odot \mathbf{R})^{-1} \mathbf{A}^{(2)}(x, \lambda)(\mathbf{R} \odot \mathbf{R}), \end{aligned}$$

from which it follows that

$$\mathbf{A}^{(2)}(x, \lambda)(\mathbf{R} \odot \mathbf{R}) = -(\mathbf{R} \odot \mathbf{R})\mathbf{A}^{(2)}(-x, \lambda). \quad (3.17)$$

Hence if $\mathbf{A}(x, \lambda)$ is reversible with reversor \mathbf{R} , the induced matrix $\mathbf{A}^{(2)}(x, \lambda)$ is reversible with reversor $\mathbf{R} \odot \mathbf{R}$. The generalization to $n > 2$ follows a similar argument.

4. Maslov angle – a formula on $\bigwedge^n(\mathbb{R}^{2n})$

The Maslov angle for a path of Lagrangian subspaces is defined in (2.7) in terms of a Lagrangian plane. For the computation, a formula in terms of the exterior algebra representation is needed. It is derived as follows.

A Lagrangian frame can be partitioned into two $n \times n$ blocks as in (2.4) and it can be represented in terms of its columns

$$\mathbf{W} = [\mathbf{w}_1 \mid \cdots \mid \mathbf{w}_n], \quad \text{with } \langle \mathbf{J}\mathbf{w}_i, \mathbf{w}_j \rangle = 0, \quad \text{for } i, j = 1, \dots, n.$$

The exterior algebra representation of the Lagrangian plane is then just obtained by the mapping

$$(\mathbf{w}_1, \dots, \mathbf{w}_n) \mapsto \mathbf{w}_1 \wedge \cdots \wedge \mathbf{w}_n \in \bigwedge^n(\mathbb{R}^{2n}).$$

Denote the exterior algebra representation by

$$\mathbf{Z} = \mathbf{w}_1 \wedge \cdots \wedge \mathbf{w}_n,$$

and orient \mathbb{R}^{2n} with the standard orientation: $\text{vol} = \mathbf{e}_1 \wedge \cdots \wedge \mathbf{e}_{2n}$.

Proposition 1. *There exists a constant n -form \mathbf{C} ,*

$$\mathbf{C} = \mathbf{C}_1 + i\mathbf{C}_2, \quad \text{with } \mathbf{C}_1, \mathbf{C}_2 \in \bigwedge^n(\mathbb{R}^{2n}),$$

such that

$$\det[\mathbf{U} - i\mathbf{V}]\text{vol} = \mathbf{C} \wedge \mathbf{Z}.$$

It follows from this proposition that there exists a scalar complex-valued function K such that $\mathbf{C} \wedge \mathbf{Z} = K\text{vol}$. A formula for the Maslov angle is then immediate.

Proposition 2.

$$e^{i\kappa} = K/\overline{K}.$$

It remains to prove Proposition 1. The proof is by explicit construction. Let

$$\mathbf{c}_j = \mathbf{e}_j - i\mathbf{J}\mathbf{e}_j, \quad j = 1, \dots, n.$$

Then

$$\begin{aligned} \mathbf{U} - i\mathbf{V} &= \begin{pmatrix} \mathbf{I} \\ -i\mathbf{I} \end{pmatrix}^T \begin{pmatrix} \mathbf{U} \\ \mathbf{V} \end{pmatrix} = [\mathbf{c}_1 \mid \cdots \mid \mathbf{c}_n]^T [\mathbf{w}_1 \mid \cdots \mid \mathbf{w}_n] \\ &= \begin{pmatrix} \langle \mathbf{c}_1, \mathbf{w}_1 \rangle & \cdots & \langle \mathbf{c}_1, \mathbf{w}_n \rangle \\ \vdots & \ddots & \vdots \\ \langle \mathbf{c}_n, \mathbf{w}_1 \rangle & \cdots & \langle \mathbf{c}_n, \mathbf{w}_n \rangle \end{pmatrix}, \end{aligned} \quad (4.1)$$

and so, using the induced inner product¹ on $\bigwedge^n(\mathbb{R}^{2n})$ (see Appendix of [4])

¹ A real inner product is used throughout the paper, with complex conjugation inserted as appropriate.

$$\det[\mathbf{U} - i\mathbf{V}] \text{vol} = \det \begin{bmatrix} \langle \mathbf{c}_1, \mathbf{w}_1 \rangle & \cdots & \langle \mathbf{c}_1, \mathbf{w}_n \rangle \\ \vdots & \ddots & \vdots \\ \langle \mathbf{c}_n, \mathbf{w}_1 \rangle & \cdots & \langle \mathbf{c}_n, \mathbf{w}_n \rangle \end{bmatrix} \text{vol} \\ = \llbracket \mathbf{c}_1 \wedge \cdots \wedge \mathbf{c}_n, \mathbf{Z} \rrbracket_n \text{vol}.$$

This gives a formula for K ,

$$K = \llbracket \mathbf{c}_1 \wedge \cdots \wedge \mathbf{c}_n, \mathbf{Z} \rrbracket_n.$$

It is not necessary to give an expression for \mathbf{C} since in the computations it is K that is needed. However, for completeness it is given. Let \mathbf{C} be an n -form satisfying

$$\mathbf{c}_1 \wedge \cdots \wedge \mathbf{c}_n \wedge \bar{\mathbf{C}} = \llbracket \mathbf{c}_1 \wedge \cdots \wedge \mathbf{c}_n, \overline{\mathbf{c}_1 \wedge \cdots \wedge \mathbf{c}_n} \rrbracket_n \text{vol}. \quad (4.2)$$

Then

$$\det[\mathbf{U} - i\mathbf{V}] \text{vol} = \mathbf{C} \wedge \mathbf{Z}.$$

The n -form \mathbf{C} is in fact the Hodge star of $\mathbf{c}_1 \wedge \cdots \wedge \mathbf{c}_n$ although the details of that characterization are not needed.

This formula generalizes the formula for the Maslov angle on $\bigwedge^2(\mathbb{R}^4)$, which is given in [1].

4.1. The Maslov angle on $\bigwedge^3(\mathbb{R}^6)$

A special case of great interest is paths of Lagrangian subspaces on \mathbb{R}^6 . The above formula can be given an explicit form. On \mathbb{R}^6 , with the standard basis, the above vectors $\mathbf{c}_1, \dots, \mathbf{c}_3$ take the form

$$\mathbf{c}_1 \wedge \mathbf{c}_2 \wedge \mathbf{c}_3 = (\mathbf{e}_1 - i\mathbf{e}_4) \wedge (\mathbf{e}_2 - i\mathbf{e}_5) \wedge (\mathbf{e}_3 - i\mathbf{e}_6) \\ = (\mathbf{e}_1 - i\mathbf{e}_4) \wedge (\mathbf{e}_2 - i\mathbf{e}_5) \wedge (\mathbf{e}_3 - i\mathbf{e}_6),$$

or

$$\mathbf{c}_1 \wedge \mathbf{c}_2 \wedge \mathbf{c}_3 = \mathbf{e}_1 \wedge \mathbf{e}_2 \wedge \mathbf{e}_3 - \mathbf{e}_1 \wedge \mathbf{e}_5 \wedge \mathbf{e}_6 \\ + \mathbf{e}_2 \wedge \mathbf{e}_4 \wedge \mathbf{e}_6 - \mathbf{e}_3 \wedge \mathbf{e}_4 \wedge \mathbf{e}_5 \\ - i\mathbf{e}_1 \wedge \mathbf{e}_2 \wedge \mathbf{e}_6 + i\mathbf{e}_1 \wedge \mathbf{e}_3 \wedge \mathbf{e}_5 \\ - i\mathbf{e}_2 \wedge \mathbf{e}_3 \wedge \mathbf{e}_4 + i\mathbf{e}_4 \wedge \mathbf{e}_5 \wedge \mathbf{e}_6.$$

Now take a standard lexical ordering for the 20-dimensional basis

$$\bigwedge^3(\mathbb{R}^6) = \text{span}\{\mathbf{e}_1 \wedge \mathbf{e}_2 \wedge \mathbf{e}_3, \mathbf{e}_1 \wedge \mathbf{e}_2 \wedge \mathbf{e}_4, \dots, \\ \mathbf{e}_3 \wedge \mathbf{e}_5 \wedge \mathbf{e}_6, \mathbf{e}_4 \wedge \mathbf{e}_5 \wedge \mathbf{e}_6\}, \quad (4.3)$$

and express an arbitrary element $\mathbf{Z} \in \bigwedge^3(\mathbb{R}^6)$ in the form $\mathbf{Z} = \sum_{i,j,k} P_{ijk} \mathbf{e}_i \wedge \mathbf{e}_j \wedge \mathbf{e}_k$. Then

$$K = \llbracket \mathbf{c}_1 \wedge \mathbf{c}_2 \wedge \mathbf{c}_3, \mathbf{Z} \rrbracket_3 = P_{123} - P_{156} + P_{246} - P_{345} - iP_{126} \\ + iP_{135} - iP_{234} + iP_{456}, \quad (4.4)$$

and so the expression for the Maslov angle is

$$e^{i\kappa} = \frac{P_{123} - P_{156} + P_{246} - P_{345} - iP_{126} + iP_{135} - iP_{234} + iP_{456}}{P_{123} - P_{156} + P_{246} - P_{345} + iP_{126} - iP_{135} + iP_{234} - iP_{456}}. \quad (4.5)$$

This formula is the basic tool for computing the Maslov index in the examples in Sections 6–8.

In this case, definition (4.2) gives

$$\mathbf{C} = \mathbf{e}_4 \wedge \mathbf{e}_5 \wedge \mathbf{e}_6 - \mathbf{e}_2 \wedge \mathbf{e}_3 \wedge \mathbf{e}_4 + \mathbf{e}_1 \wedge \mathbf{e}_3 \wedge \mathbf{e}_5 - \mathbf{e}_1 \wedge \mathbf{e}_2 \wedge \mathbf{e}_6 \\ + i(\mathbf{e}_3 \wedge \mathbf{e}_4 \wedge \mathbf{e}_5 - \mathbf{e}_2 \wedge \mathbf{e}_4 \wedge \mathbf{e}_6 + \mathbf{e}_1 \wedge \mathbf{e}_5 \wedge \mathbf{e}_6 \\ - \mathbf{e}_1 \wedge \mathbf{e}_2 \wedge \mathbf{e}_3).$$

4.2. Maslov angle on $\bigwedge^n(\mathbb{R}^{2n})$

In higher dimension, the general formula is [7]

$$K = \det(\mathbf{U} - i\mathbf{V}) \\ = \sum_{\substack{(i_1, \dots, i_n), r \\ i_1 < \dots < i_n \\ (i_1, \dots, i_r, i_{r+1}-n, \dots, i_n-n) = (1, \dots, n)}} i^{n-r} (-1)^{\sum_{j=1}^r i_j - j} P_{i_1, \dots, i_n},$$

for an element $\mathbf{Z} \in \bigwedge^n(\mathbb{R}^{2n})$ represented in terms of the standard basis:

$$\mathbf{Z} = \sum_{j_1, \dots, j_n} P_{j_1, \dots, j_n} \mathbf{e}_{j_1} \wedge \cdots \wedge \mathbf{e}_{j_n}.$$

5. Integrating on the Lagrangian Grassmannian

The strategy for numerical computation of paths of Lagrangian subspaces in the exterior algebra representation for $n > 2$ is similar to the case of $n = 2$. The major change is the jump in dimension. For example, the dimension of each of the basic manifolds for the case $n = 3$ is shown in the table below.

Manifold	$\bigwedge^3(\mathbb{R}^6)$	\mathbb{RP}^{19}	$G_3(\mathbb{R}^6)$	$\Lambda(3)$	$\Lambda^1(3)$
Dimension	20	19	9	6	5

In this table $\Lambda(3)$ is the Lagrangian Grassmannian and $\Lambda^1(3)$ is the Maslov cycle [13]. The vector space $\bigwedge^3(\mathbb{R}^6)$ has dimension 20, and we can take the standard lexical basis (4.3) and an element of $\bigwedge^3(\mathbb{R}^6)$ can be expressed in the form

$$\mathbf{Z} = \sum_{i,j,k} P_{ijk} \mathbf{e}_i \wedge \mathbf{e}_j \wedge \mathbf{e}_k, \quad i < j < k.$$

The formula for the Maslov angle is given in Eq. (4.5). For computing the Maslov index in the case where the solitary wave is approximated by a periodic orbit, the algorithm is the same as in the case of $n = 2$. Simply integrate the unstable subspace in the induced system on $\bigwedge^3(\mathbb{R}^6)$ in the interval $-L < x < +L$ with initial condition $\zeta^+(\lambda)$, where $\zeta^+(\lambda)$ is the representation on $\bigwedge^3(\mathbb{R}^6)$ of the unstable subspace at infinity. $\kappa(x, \lambda)$ is computed using (4.5) and then the Maslov index is returned at $x = L$ using (2.8). The numerical methods have been presented in previous papers: approximation of the solitary wave by a limiting periodic wave [14,15], and using an intersection theory definition of the Maslov index [1,12,16,4].

There is still much to understand about $\Lambda(3)$. For example, we do not have useful representations of $G_3(\mathbb{R}^6)$ or $\Lambda(3)$ on $\bigwedge^3(\mathbb{R}^6)$. Such representations would be advantageous for proving that $\Lambda(3)$ is an invariant manifold for (3.9), and for understanding the numerical properties of the induced ODE on $\Lambda(3)$. Some results about $\bigwedge^3(\mathbb{R}^6)$ and $\Lambda(3)$ can be found in Chapter 8 of book [17]. Nevertheless, the Maslov index is still easily computable when $n = 3$ and the calculations show evidence of robustness.

6. A model PDE for longwave–shortwave resonance

In this section, the Maslov index is computed for a class of solitary waves which arise in a model PDE for longwave–shortwave resonance (cf. [18–21]). The equations are a coupled system with one equation of nonlinear Schrödinger type and the other of KdV type. A typical form is

$$E_t = i(E_{xx} + \rho E - \nu E) \\ \rho_t = \partial_x(\rho_{xx} - c\rho + 3\rho^2 + |E|^2), \quad (6.1)$$

where $\rho(x, t)$ is real valued, $E(x, t)$ is complex valued, and c, ν are considered to be positive real parameters. In real coordinates, $E = u + iv$ and $\rho = w$, the above equations can be written as

$$u_t = -v_{xx} - vw + \nu v \\ v_t = u_{xx} + uw - \nu u \\ w_t = w_{xxx} - cw_x + 6ww_x + 2uu_x + 2vv_x. \quad (6.2)$$

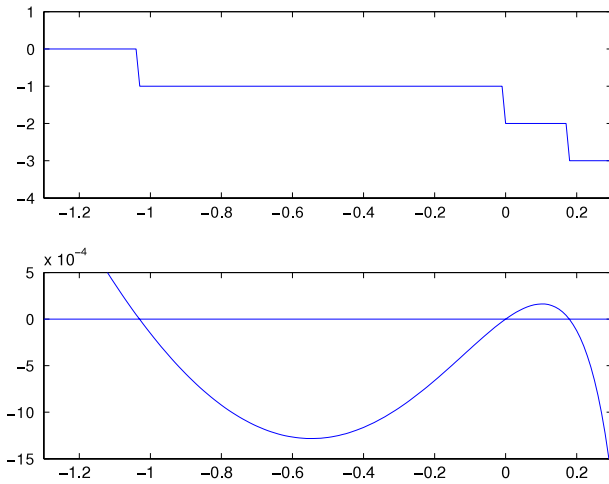


Fig. 1. Computation for the longwave–shortwave equations for the parameter values $c = 1$ and $\nu = 0.2$. Top: the Maslov index, Bottom: the Evans function.

A simplified $n = 2$ version of this example was considered in [1]. Here the full $n = 3$ example is studied.

Solitary waves satisfy the steady equations

$$\begin{aligned} -2u_{xx} - 2uw + 2\nu u &= 0 \\ -2v_{xx} - 2vw + 2\nu v &= 0 \\ -w_{xx} + cw - 3w^2 - u^2 - v^2 &= \text{constant}, \end{aligned} \quad (6.3)$$

and [19] has shown that there exist exact solutions

$$\begin{aligned} u(x) &= A \operatorname{sech}(\sqrt{\nu}x), \quad v(x) = 0 \quad \text{and} \\ w(x) &= 2\nu \operatorname{sech}^2(\sqrt{\nu}x), \end{aligned} \quad (6.4)$$

with constant = 0 and $A^2 = 2\nu(c - 4\nu)$, and the existence condition $c - 4\nu > 0$.

To study the Maslov index of these solutions, linearize the steady equations about the basic solitary wave and introduce a spectral parameter,

$$\begin{aligned} -2u_{xx} - 2\hat{w}u - 2\hat{w}w + 2\nu u &= \lambda u \\ -2v_{xx} - 2\hat{w}v - 2\hat{w}w + 2\nu v &= \lambda v \\ -w_{xx} + cw - 6\hat{w}w - 2\hat{u}u - 2\hat{v}v &= \lambda w. \end{aligned} \quad (6.5)$$

When $\hat{v} = 0$ this system decouples into a second-order equation for v (see Appendix of [1] for analysis of the reduced v equation), and a fourth-order coupled system for u, w , which can be written as a standard Hamiltonian ODE in the form (1.1) with $n = 2$ by taking

$$\mathbf{w}(x, \lambda) = \begin{pmatrix} u \\ w \\ 2u_x \\ w_x \end{pmatrix}, \quad \mathbf{B}(x, \lambda) = \begin{pmatrix} \lambda - 2\nu + 2\hat{w}(x) & 2\hat{u}(x) & 0 & 0 \\ 2\hat{u} & \lambda - c + 6\hat{w}(x) & 0 & 0 \\ 0 & 0 & \frac{1}{2} & 0 \\ 0 & 0 & 0 & 1 \end{pmatrix}.$$

The Maslov index is computed for the case $c = 1$ and $\nu = 0.2$ in [1] and the results are shown, along with the Evans function, in Fig. 1 and tabulated in the table below, where $\lambda_1 < \lambda_2 = 0 < \lambda_3$ are the three roots of the Evans function.

λ	$\lambda < \lambda_1$	$\lambda_1 < \lambda < \lambda_2$	$\lambda_2 < \lambda < \lambda_3$	$\lambda > \lambda_3$
Maslov ($\mathbf{U}^+, \mathbf{E}_\infty^-$)	0	-1	-2	-3

Now, consider the case of the full six-dimensional system (6.5). It can be reformulated in the form (1.1) by taking $\mathbf{w} =$

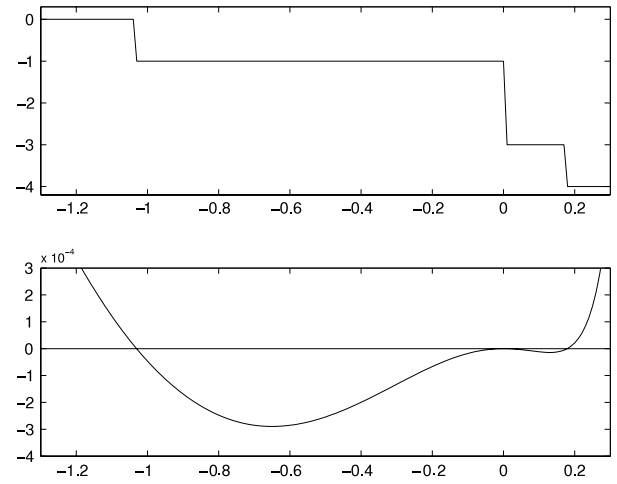


Fig. 2. Maslov index and Evans function as functions of λ associated to the 6×6 system (6.5) when $\nu = 0.2$ and $c = 1$.

$(u, v, w, 2u_x, 2v_x, w_x)$, and

$$\mathbf{B}(x, \lambda) = \begin{pmatrix} -2\nu + \lambda + 2\hat{w} & 0 & 2\hat{u} & 0 & 0 & 0 \\ 0 & -2\nu + \lambda + 2\hat{w} & 2\hat{v} & 0 & 0 & 0 \\ 2\hat{u} & 2\hat{v} & \lambda - c + 6\hat{w} & 0 & 0 & 0 \\ 0 & 0 & 0 & \frac{1}{2} & 0 & 0 \\ 0 & 0 & 0 & 0 & \frac{1}{2} & 0 \\ 0 & 0 & 0 & 0 & 0 & 1 \end{pmatrix}.$$

When $\hat{v} = 0$ the system decouples into two subsystems as noted above. In this section, the full system will be integrated on $\bigwedge^3(\mathbb{R}^6)$ for the decoupled case. This way the calculation can be checked against the previous calculation on \mathbb{R}^4 .

When a system decouples into two subsystems, the Evans function of the full system is the product of two subsystems and the Maslov index of the full system is the sum of the Maslov indexes of the two subsystems $\text{Maslov}^{2D} \oplus \text{Maslov}^{4D} = \text{Maslov}^{6D}$. Hence this formula provides a check on the calculations which are summarized below.

λ	$\lambda < -1$	$-1 < \lambda < 0$	$0 < \lambda < \approx 0.19$	$\lambda > \approx 0.19$
Maslov ^{2D}	0	0	-1	-1
Maslov ^{4D}	0	-1	-2	-3
Maslov ^{6D}	0	-1	-3	-4

In the calculations reported here, the Maslov angle in (4.5) and the algorithm in [1] are used.

Numerical results are presented in Fig. 2. The results are in complete agreement with the product of the Evans function of the subsystems and the sum of the Maslov indices of the subsystems.

As noted in Appendix D of [1] the Maslov index for the reduced system is 0 if $\lambda < 0$ and -1 if $\lambda > 0$. Adding these values to the Maslov indices in Fig. 1 agrees with the Maslov indices in Fig. 2. Note also that the Evans function has a double zero at $\lambda = 0$ as expected.

7. A triply coupled reaction–diffusion equation

Consider the coupled system of reaction–diffusion equations

$$\begin{aligned} \frac{\partial u}{\partial t} &= \frac{\partial^2 u}{\partial x^2} - 4u + 6u^2 - c_1(u - v) + c_3(w - u) \\ \frac{\partial v}{\partial t} &= \frac{\partial^2 v}{\partial x^2} - 4v + 6v^2 + c_1(u - v) - c_2(v - w) \\ \frac{\partial w}{\partial t} &= \frac{\partial^2 w}{\partial x^2} - 4w + 6w^2 + c_2(v - w) - c_3(w - u), \end{aligned} \quad (7.1)$$

where $\mathbf{c} = (c_1, c_2, c_3)$, the coupling constant, is a non-zero vector-valued real parameter. Suppose that \mathbf{c} is chosen so that the trivial solution of (7.1) is stable. This example generalizes the study of steady reaction–diffusion equations with $n = 2$ in [3,1].

This system has the exact steady solitary wave solution

$$u = v = w := \hat{u}(x) = \text{sech}^2(x).$$

Linearizing (7.1) about the basic state \hat{u} and taking perturbations of the form

$$e^{\lambda t}(u(x, \lambda), v(x, \lambda), w(x, \lambda)),$$

leads to the coupled ODE eigenvalue problem

$$\begin{aligned} u_{xx} &= (\lambda + 4 + c_1 + c_2 + c_3 - 12\hat{u}(x))u \\ &\quad - c_2 u - c_1 v - c_3 w \\ v_{xx} &= (\lambda + 4 + c_1 + c_2 + c_3 - 12\hat{u}(x))v \\ &\quad - c_1 u - c_3 v - c_2 w \\ w_{xx} &= (\lambda + 4 + c_1 + c_2 + c_3 - 12\hat{u}(x))w \\ &\quad - c_3 u - c_2 v - c_1 w, \end{aligned} \quad (7.2)$$

or

$$\mathbf{p}_{xx} = a(x, \lambda)\mathbf{p} - \mathbf{C}\mathbf{p}, \quad (7.3)$$

where

$$a(x, \lambda) = \lambda + 4 + \text{Trace}(\mathbf{C}) - 12\text{sech}^2(x),$$

and

$$\mathbf{p} = \begin{pmatrix} u \\ v \\ w \end{pmatrix} \quad \text{and} \quad \mathbf{C} = \begin{pmatrix} c_2 & c_1 & c_3 \\ c_1 & c_3 & c_2 \\ c_3 & c_2 & c_1 \end{pmatrix}.$$

This eigenvalue problem can be solved explicitly. The matrix \mathbf{C} is symmetric and so it has three real eigenvalues. Denote them by $\sigma_1, \sigma_2, \sigma_3$. Let \mathbf{T} be the 3×3 matrix whose columns are the eigenvectors of \mathbf{C} . Hence

$$\mathbf{T}^{-1}\mathbf{C}\mathbf{T} = \begin{pmatrix} \sigma_1 & 0 & 0 \\ 0 & \sigma_2 & 0 \\ 0 & 0 & \sigma_3 \end{pmatrix}.$$

The eigenvalue problem (7.3) can be diagonalized. Let $\mathbf{p} = \mathbf{T}\tilde{\mathbf{p}}$, then $\tilde{\mathbf{p}}$ satisfies

$$\begin{pmatrix} \tilde{u} \\ \tilde{v} \\ \tilde{w} \end{pmatrix}_{xx} = \begin{bmatrix} a(x, \lambda) - \sigma_1 & 0 & 0 \\ 0 & a(x, \lambda) - \sigma_2 & 0 \\ 0 & 0 & a(x, \lambda) - \sigma_3 \end{bmatrix} \begin{pmatrix} \tilde{u} \\ \tilde{v} \\ \tilde{w} \end{pmatrix}.$$

Using the result in Appendix B of [1] we can write down a formula for λ in the point spectrum. There are exactly nine eigenvalues in the point spectrum,

$$\left. \begin{aligned} \lambda_j &= -c_1 - c_2 - c_3 + \sigma_j - 3 \\ \lambda_{j+3} &= -c_1 - c_2 - c_3 + \sigma_j \\ \lambda_{j+6} &= -c_1 - c_2 - c_3 + \sigma_j + 5 \end{aligned} \right\} \quad j = 1, 2, 3.$$

The three eigenvalues of \mathbf{C} satisfy $\det[\sigma\mathbf{I} - \mathbf{C}] = 0$ or

$$\sigma^3 - (c_1 + c_2 + c_3)\sigma^2 + (c_1c_2 + c_2c_3 + c_1c_3 - c_1^2 - c_2^2 - c_3^2)\sigma + (c_1^3 + c_2^3 + c_3^3 - 3c_1c_2c_3) = 0.$$

This polynomial can be factorized. Let $\tau = \text{Trace}(\mathbf{C}) = c_1 + c_2 + c_3$. Then the above polynomial factorizes to

$$(\sigma - \tau)(\sigma^2 - \gamma^2) = 0,$$

with

$$\gamma = \frac{1}{\sqrt{2}} [(c_1 - c_2)^2 + (c_2 - c_3)^2 + (c_3 - c_1)^2]^{1/2}.$$

Hence the three σ roots are

$$\sigma_1 = \tau, \quad \sigma_2 = \gamma, \quad \sigma_3 = -\gamma.$$

This eigenvalue problem can be written in the standard form (1.1) by taking $\mathbf{w} = (u, v, w, u_x, v_x, w_x)$ and Eq. (7.4) (Box I). The matrix in (7.4) (see Box I) is Hamiltonian: $\mathbf{J}\mathbf{A}$ is symmetric.

7.1. Calculations for the case $\mathbf{c} = c(1, 1, 1)$

When $c_1 = c_2 = c_3 := c$ then $\gamma = 0$ and $\sigma_1 = 3c$, and $\sigma_2 = \sigma_3 = 0$. Hence there are nine eigenvalues

$$\{\lambda : \lambda = (-3 - 3c, -3c, -3c + 5, -3, 0, 5)\},$$

with the first three having multiplicity two. Hence the number of positive eigenvalues without multiplicity is 4, 3, 2, or 1 depending on whether $c < -1$, $-1 < c < 0$, $0 < c < 5/3$ or $c > 5/3$ respectively. According to Lemma 6 of Part 1, the Maslov index at λ counts the eigenvalues with multiplicities greater than λ , so the Maslov index can be explicitly written down:

c	$c < -1$	$-1 < c < 0$	$-1 < c < 0$	$\frac{5}{3} < c$
Maslov ^{homoclinic}	7	5	3	1

7.2. Generalization to N -coupled reaction–diffusion equations

This model can be generalized to N -coupled reaction–diffusion equations. Define

$$V(\mathbf{u}) = -\frac{1}{2} \sum_{j=1}^{N-1} c_j (u_j - u_{j+1})^2 - \frac{1}{2} c_N (u_N - u_1)^2.$$

Then the following system is a gradient reaction–diffusion system

$$\frac{\partial u_j}{\partial t} = \frac{\partial^2 u_j}{\partial x^2} - 4u_j + 6u_j^2 + \frac{\partial V}{\partial u_j}, \quad j = 1, \dots, N, \quad (7.5)$$

which generalizes (7.1) to N -coupled equations. The steady part of this equation is a Hamiltonian system on a phase space of dimension $2N$. Taking $u_j(x) = \text{sech}^2 x$ as the basic state and linearizing about it, the spectral problem can be explicitly solved in terms of the eigenvalues of the matrix \mathbf{C} . In addition, one can show in general that there is always at least one unstable eigenvalue, for any N . This follows because $\text{Trace}(\mathbf{C})$ is always an eigenvalue of the matrix \mathbf{C} with eigenvector $(1, \dots, 1)$. Model (7.5) provides a useful example for testing computational strategies for the Maslov index of Hamiltonian systems with a very large dimension.

8. A seventh-order Korteweg–de Vries equation

The KdV equation

$$u_t + uu_x + \gamma u_{xxx} = 0,$$

can be generalized by including higher-order dispersion, particularly if $|\gamma| \ll 1$, leading to the fifth-order KdV equation

$$u_t + uu_x + \gamma_1 u_{xxx} + \gamma_2 u_{xxxxx} = 0.$$

By using a systematic procedure, KdV equations of any order can be generated. When these KdV equations are derived from the water wave problem, and a Hamiltonian approximation theory is used, the resulting model equations are also Hamiltonian [22]. For many of these KdV models, solitary wave solutions have been found, both analytically (explicit solutions) and numerically.

In this section the Maslov index theory is applied to the linearization about solitary waves of the seventh-order KdV equation. There are several versions of the seventh-order KdV equation in the literature (e.g. [22–24]). The version in [23] is used here since it is Hamiltonian and has two exact solutions. The general form of the equation, called KdV7, is

$$u_t + \nu u_x + \alpha uu_x + \gamma_1 u_{xxx} + \gamma_2 u_{xxxxx} + \gamma_3 u_{xxxxxxx} = 0, \\ \gamma_1 \gamma_2 < 0.$$

$$\mathbf{A}(x, \lambda) = \begin{pmatrix} 0 & 0 & 0 & 1 & 0 & 0 \\ 0 & 0 & 0 & 0 & 1 & 0 \\ 0 & 0 & 0 & 0 & 0 & 1 \\ f(x, \lambda) + c_1 + c_3 & -c_1 & -c_3 & 0 & 0 & 0 \\ -c_1 & f(x, \lambda) + c_1 + c_2 & -c_2 & 0 & 0 & 0 \\ -c_3 & -c_2 & f(x, \lambda) + c_2 + c_3 & 0 & 0 & 0 \end{pmatrix} \quad (7.4)$$

where $f(x, \lambda) = \lambda + 4 - 12 \operatorname{sech}^2(x)$.

Box I.

By scaling u , x and t , and using the condition $\gamma_1 \gamma_2 < 0$, the KdV7 equation can be reduced to a PDE with two parameters

$$u_t - cu_x + uu_x + u_{xxx} - u_{xxxxx} + \sigma u_{xxxxxx} = 0. \quad (8.6)$$

This KdV7 equation is a simplified version of the KdV7 equation derived from the water wave problem in [22] (see page 384 in [22]). Another version of the seventh-order KdV, reported in [24], is

$$u_t + au^m u_x - bu^m u_{xxx} + u^m u_{xxxxx} + u_{xxxxxx} = 0,$$

with $m \geq 1$ and $b > 0$. It has exact solutions but does not appear to be Hamiltonian.

The KdV7 equation (8.6) can be represented in Hamiltonian form

$$u_t = \frac{\partial}{\partial x} \left(\frac{\delta \mathcal{H}}{\delta u} \right), \quad (8.7)$$

with Hamiltonian functional

$$\mathcal{H}(u) = \int_{\mathbb{R}} \left(\frac{c}{2} u^2 - \frac{1}{6} u^3 + \frac{1}{2} u_x^2 + \frac{1}{2} u_{xx}^2 + \frac{1}{2} \sigma u_{xxx}^2 \right) dx. \quad (8.8)$$

Steady solutions of KdV7, denoted by $\phi(x)$, satisfy the sixth-order ODE

$$\sigma \phi_{xxxxxx} - \phi_{xxxx} + \phi_{xx} + \frac{1}{2} \phi^2 - c\phi = 0. \quad (8.9)$$

While no theory has been worked out yet for KdV7, we expect the results for KdV5 mentioned in Part 1 linking the Maslov index to the spectral stability problem to be extendable to the KdV7 case.

In what follows, we first describe two exact solitary wave solutions and then compute their Maslov index.

8.1. Solitary wave solutions of KdV7

Solitary waves which are asymptotic to zero as $x \rightarrow \pm\infty$, correspond to homoclinic orbits of (8.9) that are homoclinic to the origin. A necessary condition for the existence of homoclinic orbits is hyperbolic eigenvalues in the system at infinity. Linearizing (8.9) about the trivial solution and looking at exponential solutions of the form $e^{\mu x}$ gives the dispersion relation

$$\Delta(\mu) = 0 \quad \text{with} \quad \Delta(\mu) := \sigma \mu^6 - \mu^4 + \mu^2 - c. \quad (8.10)$$

The roots of this polynomial are functions of c and σ , and they can be classified by plotting the discriminant in the (σ, c) plane. It is shown in Fig. 3. The discriminant is determined by the condition

$$\Delta(\mu) = \Delta'(\mu) = 0,$$

which results in

$$\sigma^2 c (243c^2 \sigma^2 + (-162\sigma + 36)c + 9(4\sigma - 1)) = 0. \quad (8.11)$$

The solution set has two branches that meet at a cusp, and are given by

$$c = \frac{9\sigma - 2 \pm 2(1 - 3\sigma)^{3/2}}{27\sigma^2} \quad \text{or} \quad \sigma = \frac{9c - 2 \mp 2(1 - 3c)^{3/2}}{27c^2}.$$

The two representations of the branches are inverse functions of each other.

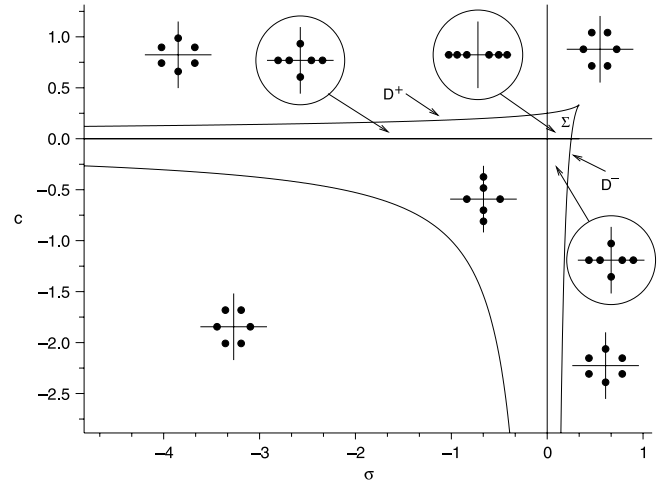


Fig. 3. The discriminant for the dispersion relation (8.10), and the qualitative position of the roots in the complex μ -plane.

Let D^+ be the branch of the discriminant with $c > 0$ and D^- the branch with $\sigma > 0$, as shown in Fig. 3. Then

$$D^\pm = \left\{ (\sigma, c) : c = \frac{9\sigma - 2 \pm 2(1 - 3\sigma)^{3/2}}{27\sigma^2} \quad \text{or} \right. \\ \left. \sigma = \frac{9c - 2 \mp 2(1 - 3c)^{3/2}}{27c^2} \right\}.$$

The cusp occurs at the point $(\sigma, c) = (\frac{1}{3}, \frac{1}{3})$ and the crossing of the σ and c axes occurs at $(\sigma, c) = (\frac{1}{4}, 0)$ and $(\sigma, c) = (0, \frac{1}{4})$. At the cusp point, the polynomial (8.10) has a pair of triple roots at $\mu = \pm 1$ since

$$\Delta(\mu) = \frac{1}{3}(\mu^2 - 1)^3 \quad \text{when} \quad (\sigma, c) = \left(\frac{1}{3}, \frac{1}{3} \right).$$

Along the line $c = 0$ the polynomial (8.10) has two zero roots, and four non-zero roots. The line $\sigma = 0$ is singular, since two of the roots disappear to infinity. The lines $c = 0$, $\sigma = 0$ and the discriminant together divide the (σ, c) plane into seven regions, and in each of these regions the position of the μ roots is qualitatively the same. The main region of interest here is the bounded region inside the discriminant and with $\sigma > 0$ and $c > 0$. It is denoted by Σ in Fig. 3. In Σ , the roots of (8.10) are all real and hyperbolic, as shown schematically in Fig. 3.

When (c, σ) is in Σ , there are two explicit solitary wave solutions of (8.9), discovered by [23]. The first one exists when

$$c = \frac{710000}{2159^2} \approx 0.1523 \quad \text{and} \quad \sigma = \frac{2159}{10000} \approx 0.2159,$$

and the explicit solution is

$$\phi(x) = a_6(\operatorname{sech}^6(kx) + \operatorname{sech}^4(kx)),$$

$$a_6 = \frac{1039500}{2159^2}, \quad k = \sqrt{\frac{25}{2159}}. \quad (8.12)$$

The other solution exists when

$$\sigma = \frac{769}{2500} \approx 0.3076 \quad \text{and} \quad c = \frac{180000}{769^2} \approx 0.3044,$$

and the explicit solution is

$$\phi(x) = a_6 \operatorname{sech}^6(kx), \quad a_6 = \frac{519750}{769^2}, \quad k = \sqrt{\frac{25}{1538}}. \quad (8.13)$$

8.2. Maslov index of solitary waves of KdV7

The Hessian of the Hamiltonian evaluated at a steady solution, $\phi(x)$, can be expressed as

$$\nabla^2 \mathcal{H}_\phi u = cu - u\phi - u_{xx} + u_{xxxx} - \sigma u_{xxxxx}.$$

Consider the following spectral problem:

$$\nabla^2 \mathcal{H}_\phi u = \lambda \phi. \quad (8.14)$$

This spectral problem is self-adjoint (in an appropriate Hilbert space) with purely real spectrum, consisting of a finite number of discrete eigenvalues and a branch of continuous spectrum. The Maslov index, which is equivalent to the Morse index in this case, can be used to count the discrete eigenvalues of this problem.

By using Legendre transform (see Appendix B of [7] for Legendre transform in this context), the system (8.14) can be represented as a linear Hamiltonian ODE.

Define

$$\mathbf{W} = \begin{pmatrix} u \\ u_{xx} - \sigma u_{4x} \\ u_{xx} \\ u_x - u_{xxx} + \sigma u_{5x} \\ -u_x \\ \sigma u_{xxx} \end{pmatrix}.$$

Then \mathbf{W} satisfies

$$\mathbf{W}_x = \mathbf{A}(x, \lambda) \mathbf{W}, \quad \text{with}$$

$$\mathbf{A}(x, \lambda) = \begin{pmatrix} 0 & 0 & 0 & 0 & -1 & 0 \\ 0 & 0 & 0 & -1 & -1 & 0 \\ 0 & 0 & 0 & 0 & 0 & 1 \\ -\lambda + c - \phi & 0 & 0 & 0 & 0 & \sigma \\ 0 & 0 & -1 & 0 & 0 & 0 \\ 0 & -1 & 1 & 0 & 0 & 0 \end{pmatrix}$$

which is Hamiltonian, with respect to the standard symplectic form, and reversible when $\phi(x)$ is an even function.

The theory for the Maslov index can now be applied to compute the index of the two solitary waves (8.12) and (8.13). The results of the computations are summarized in Figs. 4 and 5.

Qualitatively, the results are the same for the two solitary waves. They are summarized in the following table.

λ	$\lambda < \lambda_1$	$\lambda_1 < \lambda < \lambda_2$	$\lambda_2 < \lambda < \lambda_3$	$\lambda > \lambda_3$
Maslov ($\mathbf{U}^+, \mathbf{E}_\infty^s$)	0	-1	-2	-3

The value of $\lambda_2 = 0$ for both of the solitary waves. Hence, the Maslov index of the two solitary waves is $\lim_{\lambda \rightarrow 0^+} \text{Maslov}(\mathbf{U}^+, \mathbf{E}_\infty^s) = -2$.

Although the phase space dimension is larger, these Maslov index results are very similar to the results for the single-pulse solutions of the fifth-order KdV in [1].

9. Ortho-symplectic integration

Integration of the linear ODE (1.1) restricted to an exterior algebra space is very effective and robust. However, the dimension of

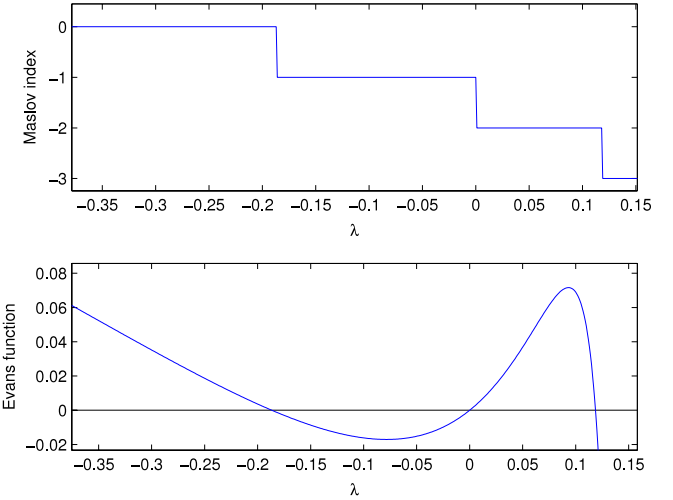


Fig. 4. Maslov index and Evans function of solution (8.12) of the seventh-order Korteweg-de Vries equation.

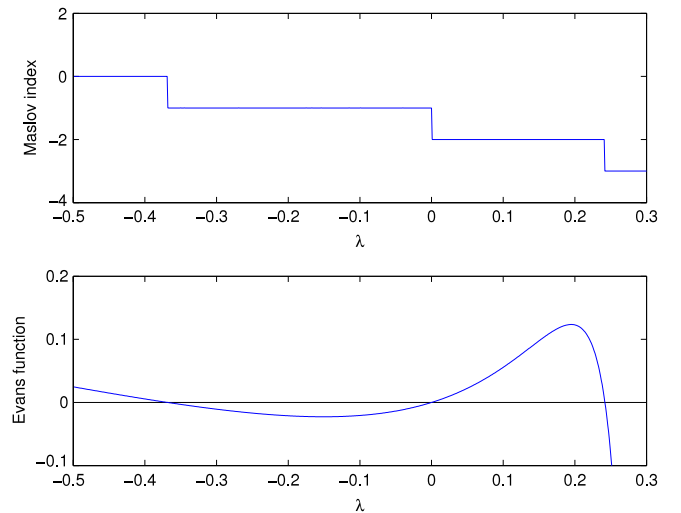


Fig. 5. Maslov index and Evans function of solution (8.13) of the seventh-order Korteweg-de Vries equation.

$\bigwedge^n(\mathbb{R}^{2n})$ equals the binomial coefficient which increases rapidly with dimension. For higher-dimensional systems an alternative to exterior algebra is continuous or discrete orthogonalization. Continuous orthogonalization has been shown to be very effective for computing the Evans function for the linearization about solitary waves [25,26], and continuous orthogonalization has been used in the Hamiltonian context for computing Lyapunov exponents [27]. The purpose of this section is to report on some experiments on the use of discrete orthogonalization for computing the Maslov index. The numerical results on the computation of the Maslov index for the solitary waves of KdV7 in Section 8 are repeated using orthogonalization.

Here the simplest form of orthogonalization is used, based on the “economy QR” algorithm in MATLAB: at each step of numerical integration, a QR factorization of the matrix \mathbf{W} is computed. Given $\mathbf{W}(x, \lambda)$, with (x, λ) fixed, there exists an upper triangular $n \times n$ -matrix \mathbf{R} and a $2n \times n$ matrix \mathbf{Q} such that $\mathbf{Q}^T \mathbf{Q} = \mathbf{I}$ and $\mathbf{W} = \mathbf{QR}$. When $\mathbf{W} \in \Lambda(n)$ then $\mathbf{Q}_1 + i\mathbf{Q}_2$ is a unitary matrix, where

$$\mathbf{Q} := \begin{pmatrix} \mathbf{Q}_1 \\ \mathbf{Q}_2 \end{pmatrix}.$$

To compute the Maslov index and the associated Evans function, the following algorithm is applied.

- (1) Fix λ and choose a large enough $L > 0$ for the integration interval $-L < x < +L$.
- (2) Compute the eigenvalues of $\mathbf{B}_\infty(\lambda)$ with positive real part and their associated eigenvectors and use them to initialize the matrix $\mathbf{W}(-L, \lambda)$ to a matrix whose columns span the unstable space of $\mathbf{B}_\infty(\lambda)$ and let $\sigma_+(\lambda)$ be the sum of these eigenvalues. Compute similarly a matrix \mathbf{S}_0 whose columns span the stable space of $\mathbf{B}_\infty(\lambda)$.

- (3) Initialize $\kappa(-L, \lambda)$ such that

$$e^{i\kappa(-L, \lambda)} = \det((\mathbf{U}_L + i\mathbf{V}_L)^{-1}(\mathbf{U}_L - i\mathbf{V}_L)),$$

with $\tilde{\mathbf{W}}(-L, \lambda) = \begin{pmatrix} \mathbf{U}_L \\ \mathbf{V}_L \end{pmatrix}$.

- (4) Assign $\mathbf{Scale}(-L) \leftarrow 1$.

- (5) In each space step, $x \mapsto x + \Delta x$ in $[-L, L]$:

- (a) Integrate equation

$$\tilde{\mathbf{W}}_x = \mathbf{A}(x, \lambda)\tilde{\mathbf{W}}, \quad \text{over } [x, x + \Delta x]. \quad (9.15)$$

- (b) Compute the economy QR-decomposition: $\tilde{\mathbf{W}}(x + \Delta x) = \mathbf{QR}$.

- (c) Assign $\mathbf{Scale}(x + \Delta x) \leftarrow \mathbf{Scale}(x) \times \det(\mathbf{R}) \times e^{-\sigma_+(\lambda)\Delta x}$.

- (d) Assign $\tilde{\mathbf{W}}(x + \Delta x) \leftarrow \mathbf{Q}$.

- (e) Take $\kappa(x + \Delta x, \lambda)$ to be the closest real number to $\kappa(x, \lambda)$ such that

$$e^{i\kappa(x+\Delta x, \lambda)} = \frac{\det[\mathbf{U} - i\mathbf{V}]}{\det[\mathbf{U} + i\mathbf{V}]},$$

with $\mathbf{Q} = \tilde{\mathbf{W}}(x + \Delta x, \lambda) = \begin{pmatrix} \mathbf{U} \\ \mathbf{V} \end{pmatrix}$.

- (6) Return $\mathbf{Scale}(L) \times \frac{\det[\tilde{\mathbf{W}}(L, \lambda), \mathbf{S}_0]}{\det[\tilde{\mathbf{W}}(-L, \lambda), \mathbf{S}_0]}$ for the Evans function.

- (7) Return $\frac{\kappa(L, \lambda) - \kappa(-L, \lambda)}{2\pi}$ for the Maslov index.

To analyse the numerical accuracy of this algorithm, one has to use exterior algebra. If we consider $\mathbf{Y}(x) = \mathbf{Scale}(x)\tilde{\mathbf{W}}(x) \odot \cdots \odot \tilde{\mathbf{W}}(x)$, then \mathbf{Y} is consistent at the same order as the numerical scheme for the equation $\mathbf{Y}'(x) = (\mathbf{A}^{(n)}(x, \lambda) - \sigma_+(\lambda))\mathbf{Y}(x)$. As a consequence, the error analysis is the same as for the exterior algebra algorithm made in part 1. Besides, we have

$$\begin{aligned} & \mathbf{Scale}(L) \times \frac{\det[\tilde{\mathbf{W}}(L, \lambda), \mathbf{S}_0]}{\det[\tilde{\mathbf{W}}(-L, \lambda), \mathbf{S}_0]} \\ & \simeq \frac{\det[\mathbf{W}(L, \lambda), \mathbf{S}(L, \lambda)]}{e^{2\sigma_+(\lambda)L} \det[\mathbf{W}(-L, \lambda), \mathbf{S}(-L, \lambda)]} \\ & \simeq \frac{\det[\mathbf{W}(L, \lambda), \mathbf{S}(L, \lambda)]}{\lim_{M \rightarrow \infty} e^{2\sigma_+(\lambda)M} \det[\mathbf{W}(-M, \lambda), \mathbf{S}(-M, \lambda)]} \end{aligned} \quad (9.16)$$

where \mathbf{S}, \mathbf{W} are matrix solutions of (2.5) and whose columns span the stable space and the unstable space respectively.

We conclude that the Evans function is also correctly estimated.

This algorithm was tested on the seventh-order Korteweg–de Vries equation in Section 8 and it worked very well. The Grassmannian is preserved since orthogonalization is enforced at every step. However, the distance from the Lagrangian manifold must be checked. Let

$$\mathbf{D} = \begin{pmatrix} \mathbf{D}_1 \\ \mathbf{D}_2 \end{pmatrix} \in \mathbb{R}^{2n \times n},$$

be a matrix with orthonormal columns: $\mathbf{D}^T \mathbf{D} = \mathbf{I}$. Then, define $\alpha(\mathbf{D}) = \rho(\mathbf{D}^T \mathbf{J} \mathbf{D})$, where ρ denotes the spectral radius, i.e. the modulus of the biggest eigenvalue. This gives an estimation of how far \mathbf{D} is from the Lagrangian manifold. This distance does not change by a right multiplication of \mathbf{D} by an orthogonal $n \times n$ -matrix.

For the numerical integration two “off the shelf” integrators were used: the standard fourth-order Runge–Kutta method in MATLAB and the implicit midpoint method. The latter one is a

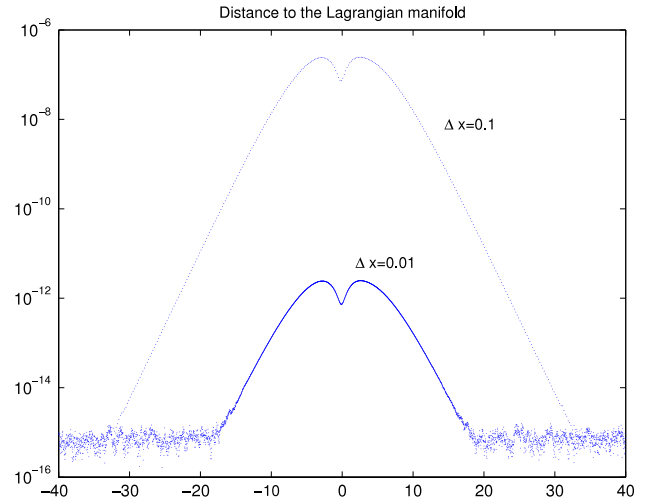


Fig. 6. Numerical test of the QR algorithm combined with the fourth-order Runge–Kutta integrator: $\alpha(\tilde{\mathbf{W}}(x))$ as a function of x for various space steps. The equation integrated is (2.3) with \mathbf{B} as in Section 8. For $\Delta x = \frac{1}{100}$, we see that the Lagrangian manifold is quite well preserved.

symplectic integrator and it preserves quadratic invariants to machine accuracy [28]. As a consequence, $\alpha(\tilde{\mathbf{W}})$ should be close to the machine precision when the implicit midpoint rule is used, and this is observed in the numerics. The error is also quite small for the Runge–Kutta method, as shown in Fig. 6, as long as the space step used is small.

The following table compares the number of operations for the exterior algebra method and the QR method.

Algorithm	Integration space	Dimension	Cost of an explicit Euler integration step	Cost of the orthogonalization step (MGS)
QR	$M_{2n,n}(\mathbb{R})$	$2n^2$	$(2n)^2 n$	$\frac{10n^3}{3}$
$2n = 4$	$M_{4,2}(\mathbb{R})$	8	32	27
$2n = 6$	$M_{6,3}(\mathbb{R})$	18	108	90
$2n = 8$	$M_{8,4}(\mathbb{R})$	32	128	214
Exterior algebra	$\bigwedge^n(\mathbb{R}^{2n})$	$\binom{2n}{n}$	$(n^2 + 1) \binom{2n}{n}$	–
$2n = 4$	$\bigwedge^2(\mathbb{R}^4)$	6	30	–
$2n = 6$	$\bigwedge^3(\mathbb{R}^6)$	20	200	–
$2n = 8$	$\bigwedge^4(\mathbb{R}^8)$	70	1190	–

So, the cost of the exterior algebra algorithm is lower for $2n = 4$, while the two algorithms are similar for $2n = 6$, with probably a slight advantage for QR. For $2n > 6$, QR is much better (one may further improve speed by not performing orthogonalization at every step).

10. Decomposing the Maslov angle into subangles

The Maslov angle is based on the fact that the determinant of the unitary matrix

$$\mathbf{Q} = (\mathbf{U} - i\mathbf{V})(\mathbf{U} + i\mathbf{V})^{-1},$$

associated with a Lagrangian plane \mathbf{W} , lies on the unit circle. However, this definition can be refined further since each of the eigenvalues of \mathbf{Q} also lies on the unit circle, and hence the Maslov angle can be decomposed into n subangles. Monitoring the angles separately can be useful when using the intersection theory definition of the Maslov index [1] and when studying bifurcations [12].

Denote the n eigenvalues of \mathbf{Q} by e^{ik_j} for $j = 1, \dots, n$ with each κ_j real. Then

$$e^{ik} = e^{ik_1} e^{ik_2} \dots e^{ik_n}.$$

These eigenvalues are independent of the choice of basis for the Lagrangian subspace represented by $\mathbf{W} \in \mathbb{R}^{2n \times n}$. Choosing any other representative leads to a similar matrix.

The subangles can be used to determine intersections with a reference space. For definiteness choose the reference space to be

$$\mathbf{Ref} = \begin{pmatrix} \mathbf{I} \\ \mathbf{0} \end{pmatrix} \in \mathbb{R}^{2n \times n}.$$

Suppose $\mathbf{W}(x)$ is a path of Lagrangian planes and suppose that all intersections between $\mathbf{W}(x)$ and \mathbf{Ref} are regular and one-dimensional.

At an intersection one of the eigenvalues of \mathbf{Q} is unity. For definiteness suppose it is κ_1 , and so $e^{ik_1(x_0)} = 1$. Then there is an eigenvector $\mathbf{v} \in \mathbb{R}^n$ such that

$$\mathbf{Q}(x_0)\mathbf{v} = e^{ik_1(x_0)}\mathbf{v} = \mathbf{v}.$$

If \mathbf{v} is chosen to be unitary and $\mathbf{JW}_x = \mathbf{BW}$, then

$$\left. \frac{d}{dx} \kappa(x) \right|_{x=x_0} = 2(\mathbf{W}\mathbf{v})^T \mathbf{B}(\mathbf{W}\mathbf{v}).$$

As a consequence, the sign of the intersection at x_0 with the reference space is simply given by the sign of $\kappa'(x_0)$.

10.1. Computing the subangles in the exterior algebra setting

These subangles can be computed in the exterior algebra framework: e^{ik_r} are the roots of the following polynomial:

$$P(\lambda) = \det((\mathbf{U} - i\mathbf{V}) - \lambda(\mathbf{U} + i\mathbf{V}))$$

The coefficients of P are antisymmetric multi-linear functions of \mathbf{W} . As a consequence, they can be expressed as a linear combination of the minors of \mathbf{W} .

Consider the case $n = 3$ where there are three subangles. By replacing \mathbf{U} and \mathbf{V} by $(1 - \lambda)\mathbf{U}$ and $(1 + \lambda)\mathbf{V}$ in formula (4.4), one obtains

$$\begin{aligned} P(\lambda) = & (1 - \lambda)^3 P_{123} - (1 - \lambda)(1 + \lambda)^2 P_{156} \\ & + (1 - \lambda)(1 + \lambda)^2 P_{246} - (1 - \lambda)(1 + \lambda)^2 P_{345} \\ & - i(1 - \lambda)^2(1 + \lambda) P_{126} + i(1 - \lambda)^2(1 + \lambda) P_{135} \\ & - i(1 - \lambda)^2(1 + \lambda) P_{234} + i(1 + \lambda)^3 P_{456}. \end{aligned} \quad (10.17)$$

This expression can be simplified to

$$P(\lambda) = -\bar{K}\lambda^3 - H\lambda^2 + \bar{H}\lambda + K,$$

where $H(\mathbf{Z}) = (-3P_{123} - P_{156} + P_{246} - P_{345} - iP_{126} + iP_{135} - iP_{234} - 3iP_{456})$.

Third-order equations are known to be solvable through Cardano's formulae. Using MAPLE, the solutions of this cubic equation are

$$\begin{aligned} e^{ik_1} = \lambda_1 = & \frac{1}{6} \frac{\Delta_1^{(1/3)}}{\bar{\mathbf{G}}} + \frac{2}{3} \Delta_2 - \frac{1}{3} \frac{\mathbf{H}}{\bar{\mathbf{G}}}, \\ e^{ik_2} = \lambda_2 = & -\frac{1}{12} \frac{\Delta_1^{(1/3)}}{\bar{\mathbf{G}}} - \frac{1}{3} \Delta_2 - \frac{1}{3} \frac{\mathbf{H}}{\bar{\mathbf{G}}} \\ & + \frac{1}{2} i \sqrt{3} \left(\frac{1}{6} \frac{\Delta_1^{(1/3)}}{\bar{\mathbf{G}}} - \frac{2}{3} \Delta_2 \right), \\ e^{ik_3} = \lambda_3 = & \frac{1}{12} \frac{\Delta_1^{(1/3)}}{\bar{\mathbf{G}}} - \frac{1}{3} \Delta_2 - \frac{1}{3} \frac{\mathbf{H}}{\bar{\mathbf{G}}} \\ & - \frac{1}{2} i \sqrt{3} \left(\frac{1}{6} \frac{\Delta_1^{(1/3)}}{\bar{\mathbf{G}}} - \frac{2}{3} \Delta_2 \right), \end{aligned}$$

$$\begin{aligned} \Delta_1 = & -36 \bar{\mathbf{H}} \mathbf{H} \bar{\mathbf{G}} + 108 \bar{\mathbf{G}} \bar{\mathbf{G}}^2 - 8 \mathbf{H}^3 \\ & + 12 \sqrt{3} \bar{\mathbf{G}} \sqrt{27 |\bar{\mathbf{G}}|^4 - |\mathbf{H}|^4} - 18 |\bar{\mathbf{G}} \mathbf{H}|^2 - 8 \operatorname{Re}(\bar{\mathbf{G}} \mathbf{H}^3), \\ \Delta_2 = & \frac{3 \bar{\mathbf{H}} \bar{\mathbf{G}} + \mathbf{H}^2}{\bar{\mathbf{G}} \Delta_1^{(1/3)}}. \end{aligned}$$

10.2. Higher dimensions and higher-dimensional intersections

Intersections between the path of Lagrangian subspaces $\mathbf{W}(x)$ and the reference space of dimension greater than one can also be considered. This case is discussed in [7]. Here a sketch of the theory is given.

There is a k -dimensional intersection at x_0 with \mathbf{Ref} if and only if there exists $S = \{r_1, r_2, \dots, r_k\} \subset \{1, \dots, n\}$ such that $e^{ik_r(x_0)} = 1$ if and only if $r \in S$.

Furthermore, if this intersection is regular, its sign is given by

$$\lim_{x \rightarrow x_0^+} \# \{r \in S | \kappa_i(x_0) \in]0, \pi[+ 2\pi \mathbb{Z}\} - \# \{r \in S | \kappa_i(x_0) \in]-\pi, 0[+ 2\pi \mathbb{Z}\}.$$

Thus, it is possible to determine the Maslov index, defined with intersections, by simply tracking the crossings of the angles κ_i with $2\pi \mathbb{Z}$.

In higher dimensions, the general expression of the polynomial $P(\lambda)$ in terms of the exterior algebra representation is

$$\begin{aligned} P(\lambda) = & \sum_{\substack{(i_1 \dots i_n, r) \\ i_1 < \dots < i_n \\ \{i_1, \dots, i_r, i_{r+1}-n, \dots, i_n-n\} = \{1, \dots, n\}}} i^{n-r} (1 - \lambda)^{n-r} \\ & \times (1 + \lambda)^r (-1)^{\sum_{j=1}^r i_j - j} \mathbf{Z}_{i_1, \dots, i_n}. \end{aligned}$$

In general the polynomial $P(\lambda)$ also satisfies the identity

$$P(\lambda) = \lambda^n P\left(-\lambda^{-1}\right).$$

References

- [1] F. Chardard, F. Dias, T.J. Bridges, On the Maslov index of solitary waves. Part 1: Hamiltonian systems on a four-dimensional phase space, *Physica D* 238 (2009) 1841–1867.
- [2] C.K.R.T. Jones, Instability of standing waves for non-linear Schrödinger-type equations, *Ergodic Theory Dynam. Systems* 8* (1988) 119–138.
- [3] A. Bose, C.K.R.T. Jones, Stability of the in-phase travelling wave solution in a pair of coupled nerve fibers, *Indiana Univ. Math. J.* 44 (1995) 189–220.
- [4] F. Chardard, F. Dias, T.J. Bridges, Computational aspects of the Maslov index of solitary waves, <http://hal.archives-ouvertes.fr/hal-00383888/en/> (2009).
- [5] J.W. Robbin, D.A. Salamon, The Maslov index for paths, *Topology* 32 (1993) 827–844.
- [6] L. Allen, T.J. Bridges, Numerical exterior algebra and the compound matrix method, *Numer. Math.* 92 (2002) 197–232.
- [7] F. Chardard, Stabilité des Ondes Solitaires, Ph.D. Thesis, École Normale Supérieure de Cachan, France, <http://tel.archives-ouvertes.fr/tel-00426266/en/> (2009).
- [8] W. Govaerts, Numerical Methods for Bifurcations of Dynamical Equilibria, SIAM, Philadelphia, 2000.
- [9] C. Stéphanos, Sur une extension du calcul des substitutions linéaires, *C.R. Acad. Sci.* 128 (1899) 593–596.
- [10] C. Stéphanos, Sur une extension du calcul des substitutions linéaires, *J. Math. Pures Appl.* 6 (1900) 73–128.
- [11] L. Allen, T.J. Bridges, Hydrodynamic stability of the Ekman boundary layer including interaction with a compliant surface: a numerical framework, *Eur. J. Mech. B/Fluids* 22 (2003) 239–258.
- [12] F. Chardard, F. Dias, T.J. Bridges, On the Maslov index of multi-pulse homoclinic orbits, *Proc. Roy. Soc. London A* 465 (2009) 2897–2910.
- [13] D. McDuff, D. Salamon, Introduction to symplectic topology, in: Oxford Mathematical Monographs, Oxford University Press, New York, 1995.
- [14] F. Chardard, F. Dias, T.J. Bridges, Fast computation of the Maslov index for hyperbolic linear systems with periodic coefficients, *J. Phys. A: Math. Gen.* 39 (2006) 14545–14557.
- [15] F. Chardard, Maslov index for solitary waves obtained as a limit of the Maslov index for periodic waves, *C. R. Acad. Sci. Paris, Ser. I* 345 (2007) 689–694.
- [16] C.-N. Chen, X. Hu, Maslov index for homoclinic orbits of Hamiltonian systems, *Ann. Inst. H. Poincaré Anal. Non Linéaire* 24 (4) (2007) 589–603.

- [17] A. Kushner, V. Lychagin, V. Rubtsov, *Contact Geometry and Nonlinear Differential Equations*, Cambridge University Press, 2007.
- [18] T. Kawahara, N. Sugimoto, T. Kakutani, Nonlinear interaction between short and long capillary-gravity waves, *J. Phys. Soc. Japan* 39 (1975) 1379–1386.
- [19] Y.C. Ma, On the multi-soliton solutions of some nonlinear evolution equations, *Stud. Appl. Math.* 60 (1979) 73–82.
- [20] E.S. Benilov, S.P. Burtsev, To the integrability of the equations describing the Langmuir-wave ion-acoustic wave interaction, *Phys. Lett. A* 98 (1983) 256–258.
- [21] A. Latifi, J. Leon, On the interaction of Langmuir waves with acoustic waves in plasmas, *Phys. Lett. A* 152 (1991) 171–177.
- [22] W. Craig, M.D. Groves, Hamiltonian long-wave scaling limits of the water-wave problem, *Wave Motion* 19 (1994) 367–389.
- [23] B.R. Duffy, E.J. Parkes, Travelling solitary wave solutions to a seventh-order generalized KdV equation, *Phys. Lett. A* 214 (5–6) (1996) 271–272.
- [24] A.-M. Wazwaz, Exact travelling wave solutions to seventh-order and ninth-order KdV-like equations, *Appl. Math. Comput.* 182 (1) (2006) 771–780.
- [25] J. Humpherys, K. Zumbrun, An efficient shooting algorithm for Evans function calculations in large systems, *Physica D* 220 (2006) 116–126.
- [26] D. Avitabile, T.J. Bridges, Numerical implementation of complex orthogonalization, parallel transport on Stiefel bundles, and analyticity, *Physica D* 239 (2010) 1038–1047.
- [27] B.J. Leimkuhler, E.S. van Vleck, Orthosymplectic integration of linear Hamiltonian systems, *Numer. Math.* 77 (1997) 269–282.
- [28] B.J. Leimkuhler, S. Reich, *Simulating Hamiltonian Dynamics*, Cambridge University Press, 2004.